Diffused Junction Depletion Layer Calculations

By H. LAWRENCE and R. M. WARNER, Jr.

(Manuscript received October 7, 1959)

Depletion layer properties have been calculated for diffused junctions in silicon and germanium as a function of reverse voltage and of diffusion parameters for the gaussian and the complementary error function distributions. These results bridge the gap between the linearly graded behavior generally exhibited by such junctions at low voltage and the step behavior exhibited at high voltage. For total depletion layer thickness and capacitance, the transition from graded to step junction behavior extends over about one decade of voltage. For depletion layer thickness on a single side of the junction, it extends over several decades. Depletion layer thickness and peak electric field are presented graphically as a function of voltage for a variety of junction depths and impurity concentration functions. The ranges for which the step and graded junction approximations are valid are apparent from these charts. The results were obtained by an analytical integration of Poisson's equation, and a subsequent use of the IBM 704 for a numerical evaluation of the transcendental equations obtained.

I. INTRODUCTION

The dependence of depletion layer properties on voltage is important in the design of many semiconductor devices. Some of these properties, such as total depletion layer thickness, are accurately predicted by the commonly used step and graded junction approximations over fairly wide voltage ranges. However, the ranges in which the approximations are applicable have not been established previously. The present work establishes the regions in which these approximations are valid and supplies data for the entire voltage range of interest.

Both the complementary error function distribution and the gaussian distribution have been treated. Total depletion layer thickness, peak electric field, capacitance per unit area and the fraction of the depletion layer on each side of the junction have been calculated for wide ranges of voltage, junction depth, background impurity concentration and

surface concentration. Results are given for silicon and germanium and can readily be extended to other materials.

II. METHOD — COMPLEMENTARY ERROR FUNCTION DISTRIBUTION

For the case of diffusion into a semiconductor with the assumption of a concentration-independent diffusion constant and a constant volume-concentration at the surface, the solution of the one-dimensional diffusion equation is the complementary error function.[1] The solution may be written

$$C(x) = C_0 \operatorname{erfc} \frac{x}{\sqrt{4Dt}}, \tag{1}$$

where C is the impurity density at a distance x from the surface, C_0 the surface concentration, D the temperature-dependent diffusion constant and t the time of diffusion.*

For the purpose of these calculations we have taken the case of a donor diffusion into a p-type semiconductor. To treat the depletion layer formed at the junction, when reverse bias is applied, we have made the following customary assumptions:

i. ionization of donors and acceptors is complete;

ii. the depletion layer is a region completely free of carriers separated by a sharp boundary from an electrically neutral region.

The net density of positive charge, ρ, lying within the depletion layer can be written

$$\rho = q(C - C_B), \tag{2}$$

where q is the electronic charge and C_B is the background impurity concentration. Hence Poisson's equation can be written in MKS units as follows:

$$\nabla^2\psi = -\frac{q}{\kappa\epsilon_0}\left(C_0 \operatorname{erfc} \frac{x}{\sqrt{4Dt}} - C_B\right), \tag{3}$$

where ψ is electrostatic potential, κ is the dielectric constant of the material and ϵ_0 is the permittivity of free space.

As Fig. 1 indicates, the electric field vanishes at the depletion layer boundaries. Thus, by integrating Poisson's equation, we can write

---

* $\operatorname{erfc} u = 1 - \operatorname{erf} u; \quad \operatorname{erf} u = \frac{2}{\sqrt{\pi}} \int_0^u \exp(-\alpha^2)\, d\alpha.$

expressions for the field distribution on the two sides of the junction: On the left,

$$E_1(x) - E_1(x_j - a_1) = E_1(x) = \frac{qC_0}{\kappa\epsilon_0}\int_{x_j-a_1}^{x}\left(1 - \frac{C_B}{C_0} - \operatorname{erf}\frac{x}{\sqrt{4Dt}}\right)dx \tag{4}$$

and, on the right,

$$E_2(x_j + a_2) - E_2(x) = -E_2(x) = \frac{qC_0}{\kappa\epsilon_0}\int_{x}^{x_j+a_2}\left(1 - \frac{C_B}{C_0} - \operatorname{erf}\frac{x}{\sqrt{4Dt}}\right)dx, \tag{5}$$

where x_j, the junction depth, is defined by

$$C_0 \operatorname{erfc}\frac{x_j}{\sqrt{4Dt}} - C_B = 0. \tag{6}$$

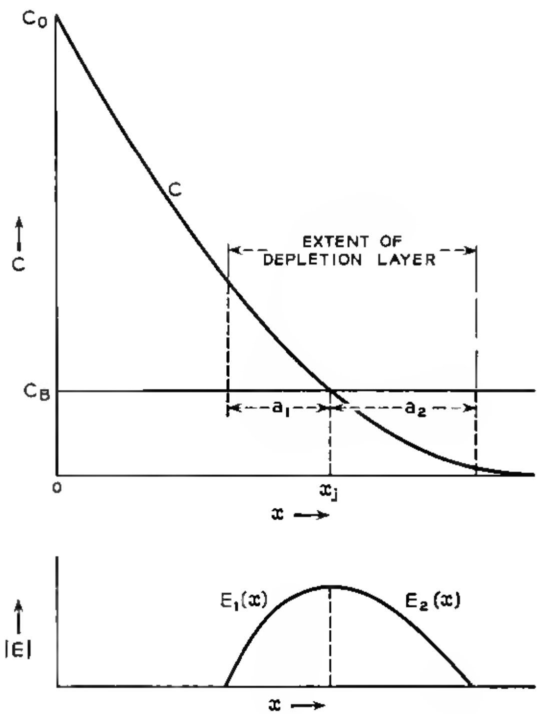

Fig. 1 — Diffusion profile and corresponding electric field distribution.

Requiring that the field be continuous at the junction enables us to arrive at the desired relation between the two components of depletion layer thickness, a_1 and a_2. That is,

$$E_1\left(x_j, \frac{C_B}{C_0}, a_1\right) = E_2\left(x_j, \frac{C_B}{C_0}, a_2\right). \tag{7}$$

At this point specific values can be chosen for x_j, C_B/C_0 and a_1 so that a_2 can be calculated by a machine using iterative methods.

Next, the voltage drops on the two sides of the junction are obtained by a second analytical integration of Poisson's equation:

$$V_1 = -\int_{x_j-a_1}^{x_j} E_1(x)\, dx, \tag{8}$$

$$V_2 = -\int_{x_j}^{x_j+a_2} E_2(x)\, dx. \tag{9}$$

For the situation chosen, reverse bias implies a positive voltage on the left-hand side with respect to the right. Therefore, the positive x direction is in the direction of decreasing voltage, and the calculated voltages are negative.

The integrations in (4), (5), (8) and (9) are carried out in detail in Appendix A.

Finally, junction capacitance is calculated from

$$C = \frac{\kappa\epsilon_0}{a_1 + a_2}. \tag{10}$$

III. METHOD — GAUSSIAN DISTRIBUTION

For the case of a diffusion having as a boundary condition that a fixed amount of the diffusant is deposited in the surface from which the diffusion proceeds, the solution of the one-dimensional diffusion equation is the gaussian function

$$C = C_0 e^{-x^2/(4Dt)}, \tag{11}$$

with the symbols being defined in the preceding section.

Again we take the case in which the donors are diffused into a p-type semiconductor, and make the same assumptions as before. For this case, Poisson's equation can be written as follows:

$$\nabla^2\psi = \frac{qC_0}{\kappa\epsilon_0}\left[e^{-x^2/(4Dt)} - \frac{C_B}{C_0}\right]. \tag{12}$$

By integrating Poisson's equation as before we can write expressions for the field distribution on the two sides of the junction:
On the left,

$$E_1(x) - E_1(x_j - a_1) = E_1(x) = \frac{qC_0}{\kappa\epsilon_0}\int_{x_j-a_1}^{x}\left[e^{-x^2/(4Dt)} - \frac{C_B}{C_0}\right]dx \quad (13)$$

and, on the right,

$$E_2(x_j + a_2) - E_2(x) = -E_2(x) = \frac{qC_0}{\kappa\epsilon_0}\int_{x}^{x_j+a_2}\left[e^{-x^2/(4Dt)} - \frac{C_B}{C_0}\right]dx, \quad (14)$$

where x_j, the junction depth, is defined by

$$[C_0 e^{-x_j^2/(4Dt)} - C_B] = 0. \quad (15)$$

Requiring that the field be continuous at the junction enables us to arrive once again at the desired relation between the two components of depletion layer thickness, a_1 and a_2. This equation, (7), is treated by machine as before.

Next, the voltage drops on the two sides of the junction are obtained by the second analytical integration of Poisson's equation, as indicated in (8) for the left side and (9) for the right side.

The integrations that yield expressions for $E_1(x)$, $E_2(x)$, V_1 and V_2 are completed in Appendix B.

In this work, values of 16.00 and 12.00 were used for the dielectric constants of germanium and silicon respectively. A simple multiplication enables one to determine field, voltage or capacitance for any modification of values of these constants, or for other materials.

The IBM 704 was employed for solving the field continuity equation (7) and for performing all the numerical computations.

IV. DATA PRESENTATION

Fig. 2 is a diagram showing total depletion layer thickness versus voltage for three kinds of impurity distributions in silicon: step with large concentration on one side, linear graded, and complementary error function. Using gaussian results instead of complementary error function results would give qualitatively the same picture. The relationship is shown for two junction depths: $x_j = 2 \times 10^{-3}$ cm and $x_j = 10^{-4}$ cm. The surface concentration is 10^{20} atoms/cm^3, and the background impurity concentration is 10^{16} atoms/cm^3. The solid curves marked "erfc," which were obtained from the calculated data, clearly mark the transi-

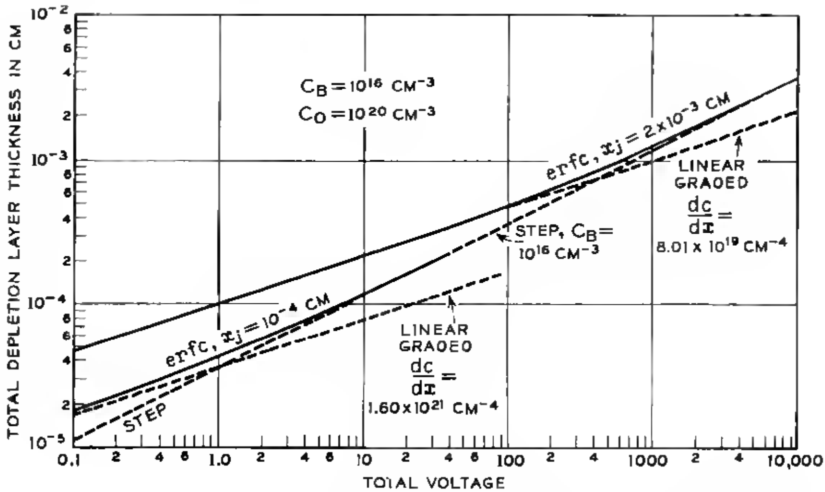

Fig. 2 — Total depletion layer thickness vs. voltage for step, linear graded and complementary error function impurity distributions in silicon.

tion region between the step and linear distributions, becoming asymptotic to these two curves at the higher and lower voltages respectively. It should be noted that, since the step junction curve is a function of background resistivity only, it remains the same for both junction depths.

The intersection of the linear graded and the step junction lines is the point where the accuracy of either approximation is poorest. Increasingly larger errors occur, of course, if either approximation is used for voltages beyond its point of intersection with the other approximation. The curves shown here constitute extreme examples. For $x_j = 10^{-4}$ cm the step junction approximation becomes excellent at about 4 volts, and hence the step approximation can be used over almost the entire voltage range of interest. In the case of $x_j = 2 \times 10^{-3}$ cm, however, breakdown occurs around 100 volts, and therefore the graded approximation is good over almost the entire voltage range of interest.

Fig. 3 presents total depletion layer thickness versus the ratio of voltage to background impurity concentration. Fig. 4 presents the corresponding data for the gaussian distribution. These charts are available for a wide range of values of the ratio C_B/C_0 ; a complete set will be furnished by the authors upon request.

The chart in Fig. 3 is precise for $C_B/C_0 = 10^{-5}$, but one may use the chart for a range from 3×10^{-6} to 3×10^{-5}. Maximum errors resulting

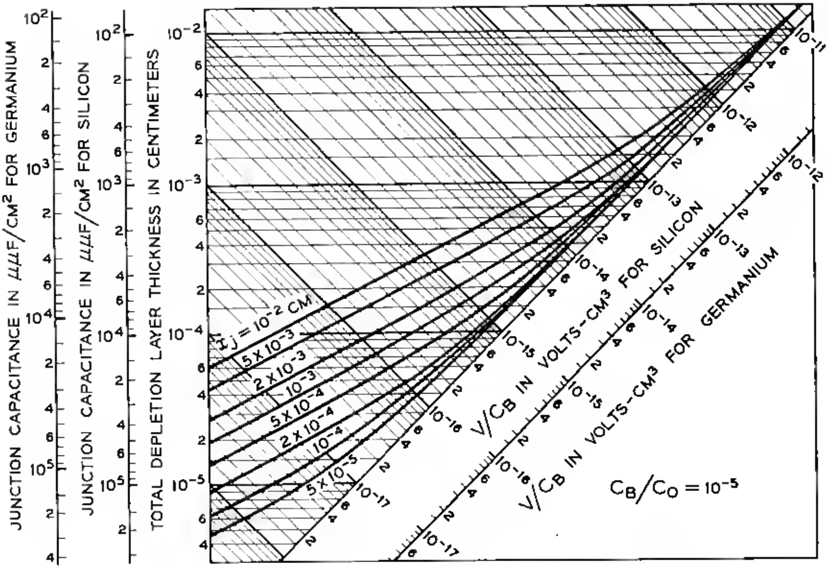

Fig. 3 — Chart for use in range 3×10^{-6} to 3×10^{-5}, erfc distribution.

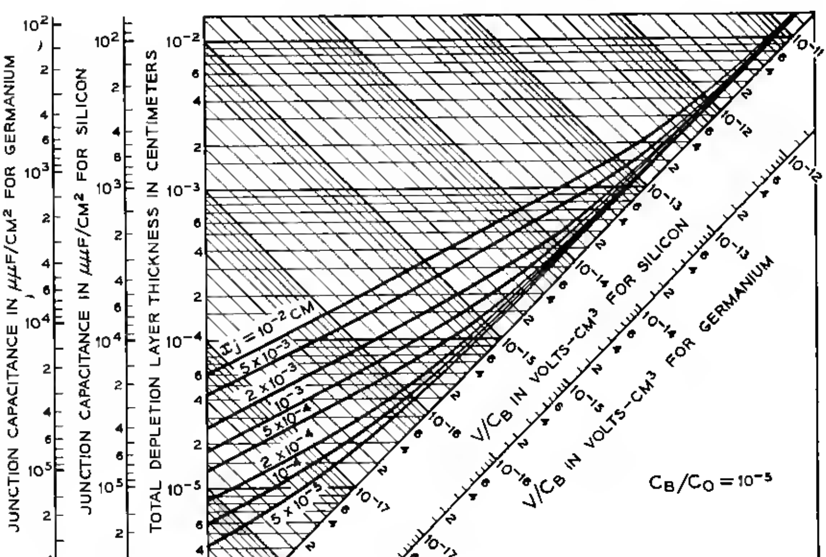

Fig. 4 — Chart for use in range 3×10^{-6} to 3×10^{-5}, gaussian distribution.

from the use of Fig. 3 over this range are 5 per cent if one wishes to obtain total depletion layer thickness for a specific value of voltage. A maximum error of 10 per cent in voltage may result when starting from a given value of total depletion layer thickness. These maximum errors apply for tbe complete set of grapbs. It can thus be seen that the use of a particular graph allows one to shift values of C_B and C_0 as long as the ratio C_B/C_0 falls within the specified range, and that, by using the complete set of graphs, one can find applicable data for any value of C_B with its corresponding C_0.

As an example, if one bas a ratio of $C_B/C_0 = 2 \times 10^{-5}$ with $C_B = 10^{15}$, one would select the chart applicable for the range 3×10^{-6} to 3×10^{-5} (Fig. 3). One can then note that the voltage reading of one volt is obtained at $V/C_B = 10^{-15}$. Then, for 10 volts, $V/C_B = 10^{-14}$ and $x_j = 2 \times 10^{-3}$, one obtains a total depletion layer tbickness of 4.7×10^{-4} cm.

The plotted data yield parallel straight lines in the left-hand portion of each chart. These lines correspond to the graded junction approximation, witb each line representing a particular gradient. At high voltages, the lincs tben converge onto the single straight line that corresponds to the step junction approximation. Thus, these charts define clearly the applicability ranges of the two approximations insofar as total layer thickness and capacitance are concerned. Oblique axes have been used to spread the curves conveniently.

Since V/C_B is used as a parameter in the charts, avalanche breakdown data cannot be readily superimposed. Tbe problem can be appreciated by noting that breakdown voltage depends on background doping in a step junction, but all step junction data have been collapsed onto a single line in these charts.

Fig. 5 shows the variation of a_1/a_{total} with the voltage function for the complementary error function distribution. Fig. 6 gives the corresponding curves for the gaussian function. The upper boundary of each chart corresponds to the graded junction, and the lower boundary corresponds to the step junction. Note that here the transition range covers many decades.

A plot of the peak electric field divided by C_B versus V/C_B is given in Fig. 7. This chart was made for $C_B/C_0 = 10^{-5}$, for the case of the complementary error function. The usefulness of the chart can be extended to include a range of C_B/C_0 from 10^{-4} to 10^{-8}, where tbe maximum error for a C_B/C_0 other than 10^{-5} is 10 per cent and, in the majority of cases, the error would be less than 5 per cent. For the gaussian distribution, the usable range of this same graph is from $C_B/C_0 = 10^{-4}$ to $C_B/$

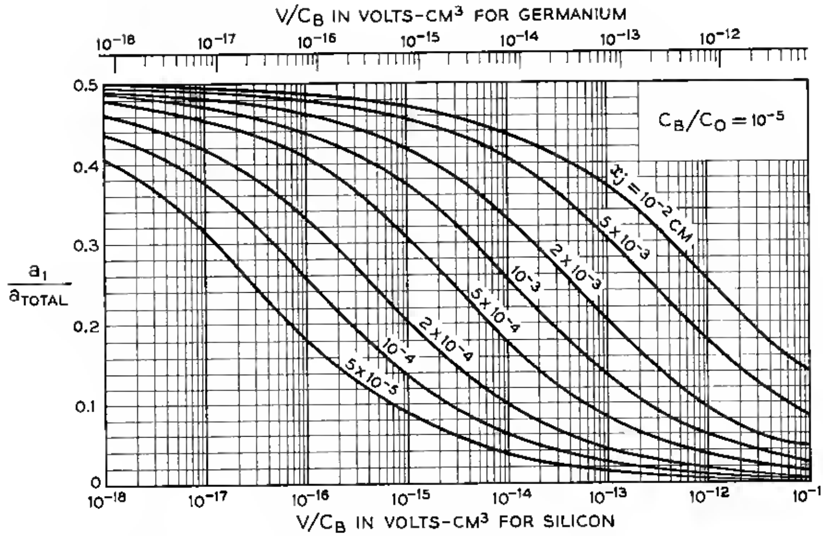

Fig. 5 — Chart for use in range 3×10^{-6} to 3×10^{-5}, erfc distribution.

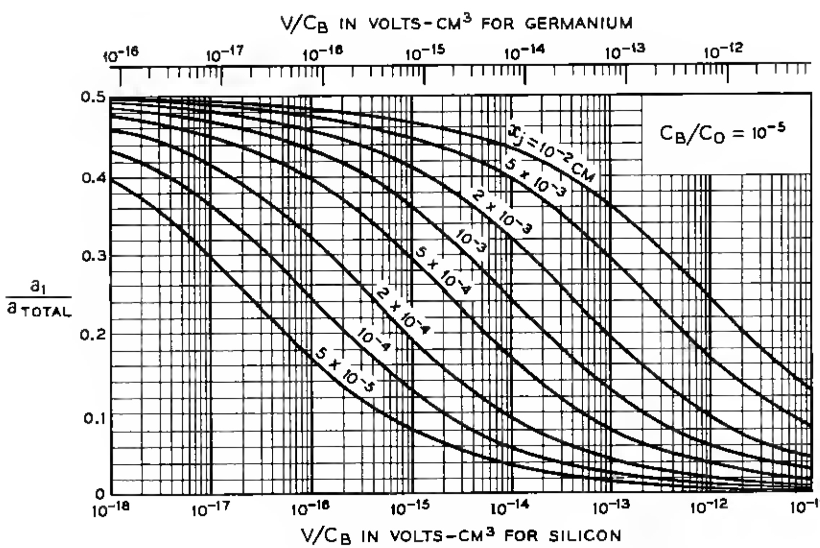

Fig. 6 — Chart for use in range 3×10^{-6} to 3×10^{-5}, gaussian distribution.

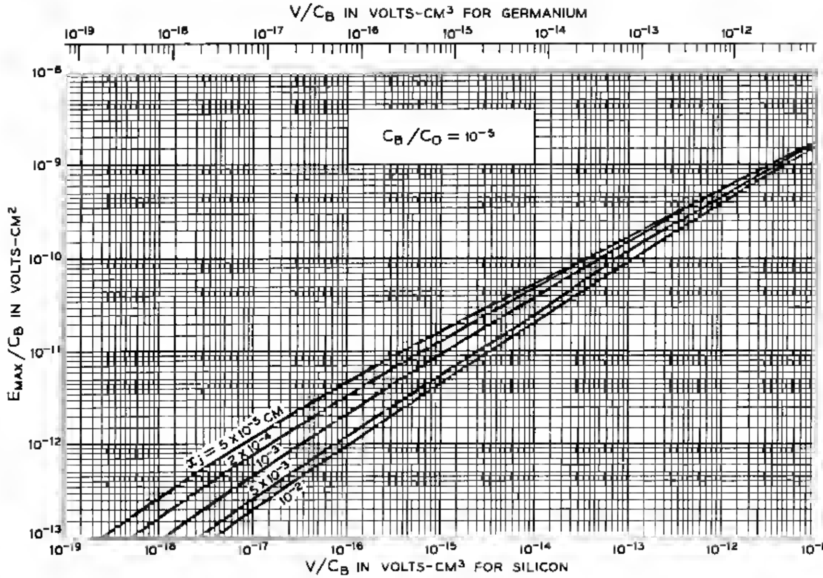

Fig. 7 — Peak electric field.

$C_0 = 10^{-6}$, with $C_B = 10^{14}$ and with errors of the same magnitude as mentioned above.

V. CONCLUSIONS

For any given diffused junction there is a voltage below which the graded approximation is excellent and a voltage about a decade higher above which the step approximation is excellent for predicting total depletion layer thickness and capacitance. It can be seen from Fig. 2 that rapidly increasing errors are introduced when either approximation is used beyond its applicable range.

The approximations are less useful in predicting the division of depletion layer thickness between the two sides of the junction, for Figs. 5 and 6 show that this transition region occurs over most of the voltage range of interest. The reason for this difference, of course, lies in the following consideration: As voltage across a diffused junction is increased, a_1 becomes smaller than the half thickness predicted by the graded approximation, and a_2 becomes larger. Thus, some compensation occurs when total thickness, $a_1 + a_2$, is computed.

The results obtained here are immediately applicable to the calculation of collector capacitance for junction transistors and junction capacitor design and the like. In field effect device design, where single-side depletion layer thicknesses are important, the results are particularly

helpful. Further, they should provide additional information for the detailed study of problems such as avalanche breakdown.

VI. ACKNOWLEDGMENT

This work would not have been possible without the patient help provided by Mrs. Wanda Mammel of the mathematical research department, who prepared the error function subroutine for the IBM 704 and contributed a great deal towards the programming of our problem. Many thanks are due also to George Levenbach for many helpful discussions and for introducing us to the IBM 704. In addition, we wish to thank all the others whose interest and suggestions have contributed to this work.

APPENDIX A

As shown in Section II, we must solve Poisson's equation, which in this case can be written

$$\nabla^2\psi = -\frac{qC_0}{\kappa\epsilon_0}\left(1 - \frac{C_B}{C_0} - \operatorname{erf}\frac{x}{\sqrt{4Dt}}\right). \tag{16}$$

All the symbols are defined as before. From (4) we have, for the electric field distribution on the left side of the junction,

$$E_1(x) = \frac{qC_0}{\kappa\epsilon_0}\int_{x_j-a_1}^{x}\left[\left(1 - \frac{C_B}{C_0}\right) - \operatorname{erf}\frac{x}{\sqrt{4Dt}}\right]dx, \tag{17}$$

and, from (5), for the right side,

$$E_2(x) = \frac{qC_0}{\kappa\epsilon_0}\int_{x_j+a_2}^{x}\left[\left(1 - \frac{C_B}{C_0}\right) - \operatorname{erf}\frac{x}{\sqrt{4Dt}}\right]dx, \tag{18}$$

where x_j, a_1 and a_2 are defined in Fig. 1.

Integrating (17) by parts, we obtain

$$\begin{aligned} E_1(x) = \frac{qC_0}{\kappa\epsilon_0}\Bigg\{&\left[\left(1 - \frac{C_B}{C_0}\right)x - x\operatorname{erf}\frac{x}{\sqrt{4Dt}} - \sqrt{\frac{4Dt}{\pi}}\, e^{-x^2/(4Dt)}\right] \\ &- \left[\left(1 - \frac{C_B}{C_0}\right)(x_j - a_1) - (x_j - a_1)\operatorname{erf}\frac{x_j - a_1}{\sqrt{4Dt}} \right. \\ &\left.\left. - \sqrt{\frac{4Dt}{\pi}}\, e^{-(x_j-a_1)^2/(4Dt)}\right]\right\}. \end{aligned} \tag{19}$$

Peak field will exist at the junction. Letting $x = x_j$ in this expression and noting that

$$1 - \frac{C_B}{C_0} = \operatorname{erf}\frac{x_j}{\sqrt{4Dt}}, \tag{20}$$

we can write for the peak field

$$E_1(x_j) = \frac{qC_0}{\kappa\epsilon_0}\left\{(x_j - a_1)\left(\operatorname{erf}\frac{x_j - a_1}{\sqrt{4Dt}} - \operatorname{erf}\frac{x_j}{\sqrt{4Dt}}\right) - \sqrt{\frac{4Dt}{\pi}}\left[e^{-x_j^2/(4Dt)} - e^{-(x_j-a_1)^2/(4Dt)}\right]\right\}. \tag{21}$$

For the range of arguments used in these calculations, the error function is very close to unity, e.g., 0.99999980. Because the IBM 704 can handle at most eight decimal digits, it is advantageous to work with the error function complement. Making this substitution, the final expression for peak field becomes

$$E_1(x_j) = \frac{qC_0}{\kappa\epsilon_0}\left\{(x_j - a_1)\left(\operatorname{erfc}\frac{x_j}{\sqrt{4Dt}} - \operatorname{erfc}\frac{x_j - a_1}{\sqrt{4Dt}}\right) - \sqrt{\frac{4Dt}{\pi}}\left[e^{-x_j^2/(4Dt)} - e^{-(x_j-a_1)^2/(4Dt)}\right]\right\}. \tag{22}$$

Similarly, (18) can be integrated to give an expression for the field distribution on the right-hand side of the junction and, specifically, the peak field:

$$E_2(x_j) = \frac{qC_0}{\kappa\epsilon_0}\left\{(x_j + a_2)\left(\operatorname{erfc}\frac{x_j}{\sqrt{4Dt}} - \operatorname{erfc}\frac{x_j + a_2}{\sqrt{4Dt}}\right) - \sqrt{\frac{4Dt}{\pi}}\left[e^{-x_j^2/(4Dt)} - e^{-(x_j+a_2)^2/(4Dt)}\right]\right\}. \tag{23}$$

The desired relation between a_1 and a_2 can be obtained by noting that field continuity requires

$$E_1(x_j) = E_2(x_j). \tag{24}$$

Thus, we obtain an equation in a_2,

$$F(a_2) = 0, \tag{25}$$

which will be solved by trial and error. From (22) and (23) it is evident that

$$\begin{aligned} F(a_2) = {} & a_2 \operatorname{erfc}\frac{x_j}{\sqrt{4Dt}} - (x_j + a_2)\operatorname{erfc}\frac{x_j + a_2}{\sqrt{4Dt}} \\ & + \sqrt{\frac{4Dt}{\pi}}\, e^{-(x_j+a_2)^2/(4Dt)} - \left[(a_1 - x_j)\operatorname{erfc}\frac{x_j - a_1}{\sqrt{4Dt}}\right. \\ & \left. - a_1 \operatorname{erfc}\frac{x_j}{\sqrt{4Dt}} + \sqrt{\frac{4Dt}{\pi}}\, e^{-(x_j-a_1)^2/(4Dt)}\right]. \end{aligned} \tag{26}$$

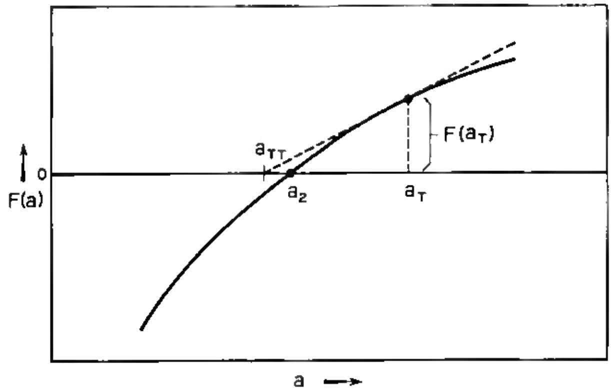

Fig. 8 — Method of obtaining approximation a_{TT} .

For rapid convergence on a_2 in the machine solution of (25), Newton's approximation was used.* For a trial value, a_T , which is a first approximation to a_2 , we simply set $a_T = a_1$. By referring to Fig. 8 it can be seen that the next approximation, a_{TT} , can be obtained from

$$a_{TT} = a_T - \frac{F(a_T)}{\left.\frac{dF}{da}\right]_{a_T}}, \tag{27}$$

where

$$\left.\frac{dF}{da}\right]_{a_T} = \operatorname{erfc} \frac{x_j}{\sqrt{4Dt}} - \operatorname{erfc} \frac{x_j + a_T}{\sqrt{4Dt}}. \tag{28}$$

By substituting a_{TT} back into (27) in place of a_T (i.e., by repeated applications of Newton's approximation), rapid convergence results. A criterion of accuracy is the expression

$$\frac{E_1(x_j) - E_2(x_j)}{E_1(x_j)}, \tag{29}$$

where the approximate value of a_2 is used in evaluating $E_2(x_j)$.

To obtain the total voltage across the junction (applied + built-in), (8) and (9) of the text must be integrated. Equation (8) yields

$$\begin{aligned} V_1 = -\frac{qC_0}{\kappa\epsilon_0} \Bigg\{ \Bigg[\left(1 - \frac{C_B}{C_0}\right) \frac{x^2}{2} - \frac{x^2}{2} \operatorname{erf} \frac{x}{\sqrt{4Dt}} \\ - \sqrt{\frac{Dt}{\pi}}\, x e^{-x^2/(4Dt)} - \kappa x \Bigg]_{x_j - a_1}^{x_j} - \sqrt{\frac{Dt}{\pi}} \int_{x_j - a_1}^{x_j} e^{-x^2/(4Dt)}\, dx \Bigg\}, \end{aligned} \tag{30}$$

* This was suggested by Miss M. C. Gray.

where κ is the second square bracket of (19). Tbe last term of (24) can be written in erf form, yielding

$$Dt\left(\operatorname{erf}\frac{x_j - a_1}{\sqrt{4Dt}} - \operatorname{erf}\frac{x_j}{\sqrt{4Dt}}\right). \tag{31}$$

Substituting (31) in (30) and converting to erfc form, we obtain

$$\begin{aligned} V_1 = -\frac{qC_0}{\kappa\epsilon_0}\Bigg[&\left(Dt + \frac{x_j^2}{2} - \frac{a_1^2}{2}\right)\left(\operatorname{erfc}\frac{x_j}{\sqrt{4Dt}} - \operatorname{erfc}\frac{x_j - a_1}{\sqrt{4Dt}}\right) \\ &+ (x_j + a_1)\sqrt{\frac{Dt}{\pi}}\,e^{-(x_j-a_1)^2/(4Dt)} - x_j\sqrt{\frac{Dt}{\pi}}\,e^{-x_j^2/(4Dt)}\Bigg]. \end{aligned} \tag{32}$$

In a similar way, (9) yields

$$\begin{aligned} V_2 = \frac{qC_0}{\kappa\epsilon_0}\Bigg[&\left(Dt + \frac{x_j^2}{2} - \frac{a_2}{2}\right)^2\left(\operatorname{erfc}\frac{x_j}{\sqrt{4Dt}} - \operatorname{erfc}\frac{x_j + a_2}{\sqrt{4Dt}}\right) \\ &+ (x_j - a_2)\sqrt{\frac{Dt}{\pi}}\,e^{-(x_j+a_2)^2/(4Dt)} - x_j\sqrt{\frac{Dt}{\pi}}\,e^{-x_j^2/(4Dt)}\Bigg]. \end{aligned} \tag{33}$$

APPENDIX B

We must again obtain a solution for Poisson's equation, which in the case of the gaussian distribution can be written

$$\Delta^2\psi = \frac{qC_0}{\epsilon\epsilon_0}\left(e^{-x^2/(4Dt)} - \frac{C_B}{C_0}\right), \tag{34}$$

where the symbols are defined as before.

Integrations corresponding to those in Appendix A are carried out to obtain the electric field distribution on either side of the junction. These field functions are as follows:

$$\begin{aligned} E_1(x) = \frac{qC_0}{\kappa\epsilon_0}\Bigg[&\sqrt{\pi Dt}\left(\operatorname{erf}\frac{x}{\sqrt{4Dt}} - \operatorname{erf}\frac{x_j - a_1}{\sqrt{4Dt}}\right) \\ &- \frac{C_B}{C_0}(x - x_j + a_1)\Bigg] \end{aligned} \tag{35}$$

and

$$\begin{aligned} E_2(x) = \frac{qC_0}{\kappa\epsilon_0}\Bigg[&\sqrt{\pi Dt}\left(\operatorname{erf}\frac{x}{\sqrt{4Dt}} - \operatorname{erf}\frac{x_j + a_2}{\sqrt{4Dt}}\right) \\ &- \frac{C_B}{C_0}(x - x_j - a_2)\Bigg]. \end{aligned} \tag{36}$$

The expressions for peak field are found immediately by substituting x_j for x in (35) and (36). Setting the resulting expressions equal to each other gives an equation that establishes field continuity at the junction [(7) of the text].

Integrating (35) again gives the voltage on the left-hand side:

$$V_1 = -\frac{qC_0}{\kappa\epsilon_0}\left\{\sqrt{\pi Dt}\,x_j\left(\operatorname{erf}\frac{x_j}{\sqrt{4Dt}} - \operatorname{erf}\frac{x_j - a_1}{\sqrt{4Dt}}\right)\right.$$
$$\left. + 2Dt[e^{-x_j^2/(4Dt)} - e^{-(x_j-a_1)^2/(4Dt)}] - \tfrac{1}{2}a_1{}^2e^{-x_j^2/(4Dt)}\right\}. \tag{37}$$

Integrating (36) gives the voltage on the right hand side:

$$V_2 = \frac{qC_0}{\kappa\epsilon_0}\left\{\sqrt{\pi Dt}\,x_j\left(\operatorname{erf}\frac{x_j}{\sqrt{4Dt}} - \operatorname{erf}\frac{x_j + a_2}{\sqrt{4Dt}}\right)\right.$$
$$\left. + 2Dt[e^{-x_j^2/(4Dt)} - e^{-(x_j+a_2)^2/(4Dt)}] - \tfrac{1}{2}a_2{}^2e^{-x_j^2/(4Dt)}\right\}. \tag{38}$$

REFERENCE

1. Barrer, R. M., *Diffusion In and Through Solids*, Macmillan, New York, 1941.